Low-intensity Pulsed Ultrasound Ameliorates Angiotension Ii-induced Cardiac Fibrosisbyalleviating Inflammation via a Caveolin-1-dependent Pathway

Kun Zhao

Jiangsu Province Hospital and Nanjing Medical University First Affiliated Hospital

https://orcid.org/0000-0002-0882-9388

Jing Zhang

Jiangsu Province Hospital and Nanjing Medical University First Affiliated Hospital

Tianhua Xu

Jiangsu Province Hospital and Nanjing Medical University First Affiliated Hospital

Chuanxi Yang

Jiangsu Province Hospital and Nanjing Medical University First Affiliated Hospital

Liqing Weng

Jiangsu Province Hospital and Nanjing Medical University First Affiliated Hospital

Tingting Wu

Nanjing Medical University First Affiliated Hospital

Xiaoguang Wu

Nanjing Medical University First Affiliated Hospital

Jiaming Mao

Key Laboratory of Modern Acoustics, Department of Physics, Collaborative Innovation Center of Advanced Microstructure

Xiasheng Guo

Key Laboratory of Modern Acoustics, Department of Physics, Collaborative Innovation Center of Advanced Microstructure

Juan Tu

Key Laboratory of Modern Acoustics, Department of Physics, Collaborative Innovation Center of Advanced Microstructure

Dong Zhang

Key Laboratory of Modern Acoustics, Department of Physics, Collaborative Innovation Center of Advanced Microstructure

Bin Zhou

Department of Genetics

Wei Sun

Jiangsu Province Hospital and Nanjing Medical University First Affiliated Hospital

Xiangqing Kong (✉ 1227621374@qq.com)

Jiangsu Province Hospital and Nanjing Medical University First Affiliated Hospital

https://orcid.org/0000-0001-8245-867X

Research

Abstract

Background: Cardiac hypertrophy and fibrosis are major pathological manifestations observed in left ventricular remodeling induced by Angiotensin II (AngII). Concerning the fact that low-intensity pulsed ultrasound (LIPUS) has been reported to improve cardiac dysfunction and myocardial fibrosis in myocardial infarction (MI) through mechanotransductionanditsdownstream pathways, we aimed to investigate whether LIPUS could also exert a protective effect on ameliorating AngII-induced cardiac hypertrophy and fibrosis andand if so, to further elucidate the underlying molecular mechanisms.

Methods: In our study, we used AngII to mimic the animal and cell culture models of cardiac hypertrophy and fibrosis, where LIPUS irradiation (0.5MHz, 77.20mW/cm^2) was applied for 20 minutes every 2 days from 1 week before surgery to 4 weeks after surgery in vivo, and every 6 hours for a total of 2 times in vitro. Following that, the levels of cardiac hypertrophy and fibrosis were evaluated by echocardiographic, histopathological, and molecular biological methods.

Results: Our results showed that LIPUS irradiation could ameliorate left ventricular remodeling in vivo and cardiac fibrosis in vitro by reducing AngII-inducedrelease of inflammatory cytokines, while the protective effects were limited on cardiac hypertrophy in vitro. Given that LIPUS irradiation increased the expression of caveolin-1 related to mechanical stimulation, we inhibited caveolin-1 activity with pyrazolopyrimidine 2 (pp2) in vitro, by which LIPUS-induced downregulation of inflammation was reversed and the anti-fibrosis effects of LIPUS irradiation were absent.

Conclusions: Taken together, these results indicate that LIPUS irradiation could ameliorate AngII-induced cardiac fibrosis by alleviating inflammation via a caveolin-1-dependent pathway, providing new insights for the development of novel therapeuticapparatus in clinical practice.

Background:

As an adaptive response of the heart to various physiological or pathological stimuli, cardiac remodeling can normalize increased wall stress of the left ventricle (LV) and then result in decompensated heart failure ([1–3]). It has been considered one of the most common causes of mortality worldwide. The progression of cardiac remodeling is characterized by cardiac hypertrophy and myocardial fibrosis, which is highly related to mechanical stress and neurohumoral stimulation ([4, 5]).

Angiotensin II (AngII) is a vital octapeptide of the renin-angiotensin system (RAS), which facilitates cardiac remodeling in vivo and in vitro via key molecular mechanisms involved in the oxidative stress, cell apoptosis, and inflammatory responses ([6–9]).

It has been indicated that the release and activation of TGF-β and other transcription factors induced by AngII play crucial roles in promoting the deposition of extracellular matrix (ECM) in fibrosis, thereby mediating cardiac structural remodeling in an auto/paracrine manner ([10–12]).

Although there have been many therapeutic methods targeting the pathogenetic mechanism of pathological cardiac remodeling in the clinic, adequate and effective treatment modalities for this disease are still lacking. Therefore, it is valuable to find novel therapeutic targets for it.

In addition to the diagnostic role of ultrasound, low-intensity pulsed ultrasound (LIPUS), a safe and noninvasive method of mechanical stimulation, has been studied and widely applied to treat various diseases clinically through regulating inflammatory responses and downstream intracellular signaling pathways ([13−17]). Previous studies have revealed that LIPUS therapy could attenuate and reverse cardiac dysfunction and ameliorate myocardial fibrosis in animal models of myocardial infarction (MI) and transverse aortic constriction (TAC) through the involvement of mechanotransduction and activation of the p38 MAPK signaling pathways ([18−20]). Moreover, repetitive LIPUS irradiation also has a positive therapeutic effect not only on chronic myocardial ischemia but also on nonischemic heart diseases, such as hypertensive heart disease, through therapeutic angiogenesis and/or mediation of caveolin-1 ([19, 21]).

As an important functional protein on the cell membrane for sensing mechanical stimuli, including cell stretch induced by LIPUS irradiation, caveolin-1 is the main component of caveolae involved in the mechanotransduction process ([22−24]). It has been demonstrated that caveolin-1 is directly responsible for the physiological and pathological function of human fibroblasts through mediating the activation of various key signaling molecules and signaling pathways, such as nitric oxide synthase (NOS) and G-protein subunits ([25−29]). In addition to responding to mechanical stress by interacting with β1-integrin, recent studies have also reported that caveolin-1 can regulate inflammatory responses that contribute to fibrotic diseases via MAPK signaling ([30−34]). However, it is still unknown whether LIPUS irradiation can improve AngII-induced cardiac remodeling through caveolin-1-mediated mechanotransduction and its downstream pathways.

Thus, in our study, we aimed to investigate the effects of LIPUS irradiation on AngII-induced cardiac remodeling and to further explore the underlying molecular mechanisms.

Methods:

Animal care

All experiments with animals were conducted strictly following the University's guidelines for the Care and Use of Laboratory Animals (publicationNo.85 − 23, revised1996; National Institutes of Health, Bethesda, MD, United States) and were approved by the Committee on Use and Care of Experimental Animals of Nanjing Medical University (Nanjing, China).

Wild-type C57BL/6J male mice (4−6 weeks old) were purchased from Model Animal Research Center of Nanjing University (Nanjing, China) and housed in a temperature-controlled room with a 12 h/12 h light/dark cycle. The standard chow and tap water were given ad libitum.

Study design and Grouping

After random assignment into groups according to body weight, the mice were implanted with an ALZET 2004 osmotic mini-pump (Durect Corp, Cupertino, CA) filled with either AngII (2.5 mg $\cdot$ kg^{-1} $\cdot$ d^{-1}) or phosphate-buffered saline (PBS) subcutaneously under inhalation anesthesia with isoflurane, and the contents were delivered at the rate of 0.25 µl/h for 4 successive weeks. PBS was administered in control groups, and the infusion rate of AngII was determined according to a previous report ([35]). The treatment group and the LIPUS control group underwent LIPUS irradiation (described below) for 20 minutes under isoflurane anesthesia every 2 days from 1 week before surgery to 4 weeks after surgery. The sham group and model group underwent the same anesthesia but without LIPUS irradiation. After evaluating cardiac function by echocardiography at the end of 4 weeks, all the mice were euthanized, and heart samples were excised and weighed for follow-up studies. Thereafter, the atrium was removed, and the left ventricle was isolated. Frozen tissue samples were employed for WB and qPCR analysis, while formalin-fixed and paraffin-embedded tissue samples were used for Sirius Red staining, hematoxylin and eosin staining, Masson staining, and immunofluorescence staining.

Cell isolation and culture

Fresh neonatal rat cardiomyocytes (NRCMs) and neonatal rat cardiac fibroblasts (NRCFs) were isolated from 1 to 3-day-old newborn Sprague–Dawley rats (Vital River Biological Co., China) as previously described ([36, 37]). Then, approximately 4×10^5 NRCMs were seeded and cultured in 60-mm cell culture dishes with DMEM (Gibco Co., USA) containing 10% (v/v) horse serum (HS, Gibco Co., USA), 5% (v/v) fetal bovine serum (FBS, HyClone Co., USA), and 1% (v/v) penicillin-streptomycin (P/S, HyClone Co., USA).

On the second day of culture, NRCMs were incubated in serum-free DMEM overnight starvation before further experiments. Then, the treatment group and LIPUS control group were exposed to LIPUS irradiation for 20 minutes every 6 hours for a total of 2 times. After that, the model group and treatment group underwent induction with 1 mmol/l of AngII (Sigma-Aldrich Co., USA) for 48 hours. In some experiments, cells were preliminary incubated with 10 µmol/l of pyrazolopyrimidine 2 (pp2, S7008, Selleck Co., China) and/or 1 µM TLR4 inhibitor TAK-242 (soluble in 1‰ DMSO, Selleck Co., China) for 2–3 hours or 1 ng/ml reconstitute the lyophilized recombinant Rat Interleukin-1β (rRtIL-1β) / recombinant Rat Interleukin-6 (rRtIL-6) for 12 hours prior to LIPUS irradiation.

NRCFs were also seeded in 60-mm cell culture dishes but were cultured in fibroblast medium (FM, Sciencell Co., China); they were treated identically to NRCMs in subsequent experiments.

All these cells were subjected to WB, qPCR, ELISA, and immunofluorescence analyses.

Echocardiography

Transthoracic echocardiographic images of mice hearts were acquired at the end of 4 weeks after surgery with an ultrasound system (Vevo 3100, VisualSonics, Toronto, Canada) under isoflurane anesthesia.

Then, LV fractional shortening (LVFS), LV ejection fraction (LVEF), LV internal diameters at end systole (LVIDs), and LV internal diameters at end diastole (LVIDd) were calculated by the operator who was blinded to the grouping design of this animal experiment.

Western blotting (WB)

The isolated tissues or lysed cells were sonicated and then homogenized in RIPA lysis buffer (Beyotime Biotechnology Co., China). After centrifugation, the protein concentration of the supernatant was quantified with the BCA assay (Pierce Biotechnology, Inc., Rockford, IL, USA).

Equal amounts of proteins (30 µg) mixed with loading buffer were separated by electrophoresis using 10% SDS−PAGE and then transferred to PVDF membranes. After blocking with 5% bovine serum albumin for 2 hours at room temperature, the membranes were incubated overnight at 4°C with primary antibodies (1:1,000 dilution) against collagen I (Beyotime Biotechnology, China), α-smooth muscle actin (α-SMA, Cell Signaling Technology, USA), TGF-β (Beyotime Biotechnology, China), VEGF (Cell Signaling Technology, USA), caveolin-1 (Cell Signaling Technology, USA), and GADPH (Beyotime Biotechnology, China). Following incubation with horseradish peroxidase (HRP)-conjugated secondary antibodies (1:5000 dilution) for 2 hours at room temperature and washing in tris-buffered saline, the blots were detected with enhanced chemiluminescence reagent (ThermoFisher Co., USA) with optimal exposure time. The intensity of protein bands was analyzed and normalized to that of GAPDH by ImageJ software.

Quantitative PCR analysis

Total RNA was extracted from the isolated specimens or lysed cells by homogenizing in TRIzol (Invitrogen Life Technologies, Carlsbad, CA) following the manufacturer's instructions. A total of 0.5 mg of RNA was reverse transcribed to single-strand cDNAs by PrimeScript™ RT reagents kit (TaKaRa, Japan). Then, q-PCR was performed with Power SYBR green PCR Master Mix using a 7900HT fast real-time PCR system (Applied Biosystems, Carlsbad, CA, USA). The relative mRNA levels were expressed according to the $2^{-\Delta\Delta Ct}$ method and normalized to those of the endogenous control (GAPDH). The primer sequences are listed in Supplemental Table 1 (Additional file 1).

Low-intensity pulsed ultrasound stimulation

LIPUS irradiation was performed using an ultrasound machine including an ultrasonic generator (Agilent Technologies, Santa Clara, CA, USA), a broadband power amplifier (Verasonics, Inc., USA), and a planar transducer (Haifu, Chongqing, China). LIPUS stimulation was applied for 20 minutes at a planar transducer frequency of 0.5 MHz and an intensity of 19.30-120.63 mW/cm^2 in 10-ms pulse bursts (Additional file 2: Supplemental Table 2). The number of cycles was 100, and the spatial-temporal average sound pressure was 0.3 MPa. The 60-mm culture dishes seeded with cells were placed on the top of the transducer filled with deaerated water. In addition, we used a temperature test paper (TMCHallcrest, USA) to test the temperature of the culture media in the dishes, and the results showed that there were

hardly any changes in temperature under our ultrasound conditions during LIPUS procedures (Additional file 3: Fig. S1).

Flow cytometry

After different treatments, the collected viable cells and cell debris were incubated with propidium iodide (PI) and Annexin-V (Fcmacs Biotech Co., China) in the binding buffer away from light at room temperature for 25 minutes following the manufacturer's use instructions. Then, the flow cytometry method was applied to analyze the relative ratio of cell apoptosis.

Masson's and Sirius Red staining

After dewaxing and rehydration, 5-μm-thick formalin-fixed, paraffin-embedded tissue sections were stained with Masson's and Sirius Red staining (Service Biological Technology Co., Ltd, Wuhan, China) using standard procedures. Then, more than 3 randomly selected whole-section images were taken with a Zeiss fluorescence upright microscope (Carl Zeiss, Jena, Germany) and measured to assess the percentage of myocardial fibrosis with Image-Pro Plus software (version 6.0; Media Cybernetics, Inc., Bethesda, MD, USA).

Wheat Germ Agglutinin (WGA) and Hematoxylin–Eosin (HE) staining

To determine the area of cardiomyocyte cross-sections, the deparaffinized and rehydrated paraffin-embedded sections were stained with WGA Alexa Fluor 647 (1:500 dilution; Invitrogen Life Technologies, Carlsbad, CA) in combination with the secondary antibody and examined by HE staining (Service Biological Technology Co., Ltd, Wuhan, China) according to the provided protocols. A minimum of 5 random fields were observed and chosen by a Zeiss fluorescence upright microscope (Carl Zeiss, Jena, Germany); they were further analyzed using ImageJ software in a blinded manner.

Immunofluorescence analyses

NRCMs seeded in culture dishes were blocked with PBS containing 5% goat serum, 5% BSA, and 0.5% Triton for 1 hour at room temperature after fixation with 4% paraformaldehyde and permeabilization with 1% Triton. Then, cells were incubated with anti-actinin antibody (1:150; Sigma-Aldrich Co., USA) and caveolin-1 (Cell Signaling Technology, USA) overnight at 4 °C, followed by incubation with rabbit IgG antibody (Alexa Fluor 488) and dilution with DAPI at room temperature. After that, a Zeiss fluorescence inverted microscope was used to digitize more than 3 fields of view in each group at random. The images were blindly analyzed with Image J software.

Statistics

Data are presented as the mean ± standard error of the mean (SEM). One-way analysis of variance (ANOVA) was applied to determine statistical significance for experiments with more than two groups, followed by Bonferroni's post hoc tests (NS indicates not significant, $*P < 0.05$, $**P < 0.01$, $***P < 0.001$,

****P < 0.0001). Statistical analyses were performed using GraphPad Prism 7.0 software (GraphPad software Inc., CA, USA).

Results:

LIPUS irradiation ameliorates AngII-induced cardiac fibrosis in vitro.

To determine whether LIPUS irradiation has effects on AngII-induced cardiac hypertrophy and fibrosisin vitro, experiments were performed in rat cardiomyocytes and cardiac fibroblasts. First, flow cytometry was applied to detect the impact of different doses of ultrasound intensities on the apoptosis of cardiomyocytes and cardiac fibroblasts. The results showed that 120.63 mW/cm^2 LIPUS can promote apoptosis of both types of cells (Fig. 1a, Additional file 4: Fig. S2). Therefore, the ultrasound intensity used in further studies was no more than 77.20 mW/cm^2. Then, as shown in Fig. 1b-e, increased protein expression and mRNA levels of α-SMA, TGF-β, and collagen I in cardiac fibroblasts induced by AngII were downregulated by LIPUS irradiation in a dose-dependent manner. Furthermore, following treatment with/without LIPUS and/or AngII, immunostaining of cardiomyocytes with a-Actini was utilized to demonstrate that LIPUS irradiation could hardly inhibit AngII-induced hypertrophic growth of cardiomyocytes (Fig. 1f). Next, qPCR results showed that LIPUS irradiation could inhibit mRNA levels of atrial natriuretic peptide (ANP), B-type natriuretic peptide (BNP) in cardiomyocytes following AngII induction in a dose-dependent manner (Fig. 1g-h). However, the increased mRNA levels of β-myosin heavy chain (β-MHC), and α-myosin heavy chain (α-MHC) were not significantly ameliorated by LIPUS irradiation (Fig. 1i-j). These findings demonstrate that LIPUS could play a protective role in AngII-induced cardiac fibrosis but had a limited effect on cardiac hypertrophy in vitro. Subsequently, considering all the data shown above, cardiac fibroblasts were chosen as the main experimental subjects, and 77.20 mW/cm^2 was selected as the most suitable ultrasonic intensity for further experiments in vivo and in vitro.

LIPUS irradiation ameliorates AngII-induced cardiac hypertrophy in mice in vivo.

To examine whether established cardiac remodeling induced by chronic AngII infusion in vivo can be inhibited by LIPUS irradiation, we used an AngII-infused mouse model to investigate the effects of LIPUS (Fig. 2a). First, following AngII infusion for 4 weeks, the significant continuous weight loss in mice observed in the model group was reduced by LIPUS irradiation to a certain degree (Fig. 2b). The echocardiographic data also showed that LVFS, LVEF, and LVIDs, but not LVIDd were significantly increased in the model group compared with the control group and were ameliorated by LIPUS irradiation (Fig. 2c, Table 1). Moreover, the model group had cardiac adverse structural remodeling with grossly enlarged hearts (Fig. 2d) and increased ratios of heart weight/body weight (HW/BW) and heart weight/tibia Length (HW/TL) compared with the control group, and LIPUS irradiation partly decreased these pathological indexes (Fig. 2e-f). A similar trend was also seen in the mRNA expression of cardiac fetal genes, including ANP, BNP, β-MHC, and α-MHC, indicating a protective role of LIPUS irradiation in AngII-induced cardiac hypertrophy (Fig. 2g-j). Furthermore, we measured the cross-sectional area of

cardiomyocytes to determine the effect of LIPUS on myocyte hypertrophy by WGA and HE staining. The results of the quantitative analysis showed that LIPUS irradiation reduced the expanded myocyte cross-sectional area significantly following AngII infusion (Fig. 3a-c).

LIPUS irradiation ameliorates AngII-induced myocardial fibrosis in mice in vivo.

Fibrosis is known to result in phenotypic changes associated with pathological myocardial remodeling ([38]). Therefore, we examined the effect of LIPUS irradiation on AngII-induced myocardial fibrosis in formalin-fixed, paraffin-embedded sections using Masson and Sirius Red staining. The analysis of the total collagen content showed that marked collagen deposition in LV tissues could be visualized in the model group compared with the control group, while mice in the treatment group displayed less collagen accumulation than those in the model group (Fig. 3d-f). Furthermore, the protein expression of TGF-β, and collagen I was assessed by WB after normalization to GAPDH. We found that LIPUS irradiation could decrease the increased TGF-β, and collagen I expression following AngII administration (Fig. 3g).

In addition, there was no significant difference in any measurements of LV structure or function mentioned above in the LIPUS control group compared with the control group, as expected. These data suggested that LIPUS irradiation could attenuate and even revert cardiac hypertrophy and myocardial fibrosis in vivo.

LIPUS irradiation ameliorates AngII-induced cardiac fibrosis via caveolin-1.

As caveolin-1 has been reported to be involved in the beneficial effects of LIPUS in ameliorating postmyocardial infarction LV remodeling ([18]), we next examined the contribution of caveolin-1 in the anti-remodeling effects of LIPUS. First, immunofluorescence results showed that LIPUS irradiation but not AngII treatment increased the activation of caveolin-1 in cardiac fibroblasts in vivo and in vitro (Fig. 4a-b and Fig. 5a-b). However, no obvious difference in caveolin-1 activation was found in cardiomyocytes among groups (Fig. 4c-d and Fig. 5c-d). With regard to the frozen mice heart tissues, higher expression levels of caveolin-1 and VEGF were also found following LIPUS irradiation when compared with the control group (Fig. 4e-f). We also found that the protein and mRNA expression levels of caveolin-1 increased following LIPUS irradiation in cardiac fibroblasts (Fig. 5e-f). However, there were no differences in caveolin-1 expression observed between the control group and the model group. Subsequently, we used pp2 to suppress the expression of caveolin-1 to further investigate its contribution to the beneficial effect of LIPUS on AngII-induced cardiac fibrosis in vitro. Following pretreatment with pp2, the antifibrotic effects of LIPUS in cardiac fibroblasts (Fig. 5g-h) and its beneficial effects on downregulating the mRNA expression levels of ANP and BNP in cardiomyocytes were both reversed (Additional file 5: Fig. S3a-b). In addition, pp2 pretreatment did not significantly interfere with the pathological effect of AngII in our study.

LIPUS irradiation ameliorates AngII-induced cardiac fibrosis by alleviating inflammation via a caveolin-1-dependent pathway.

Since the inflammatory response has been evidenced to be vital in the progression of cardiac remodeling ([39]), we next investigated the mRNA expression of several proinflammatory cytokines, including TNF-α, IL-1β, and IL-6, in cardiac fibroblasts by qPCR. As shown in Fig. 6a, compared with the control group, there was a modest increase in the mRNA expression levels of TNF-α, IL-1β, and IL-6 following AngII administration, which was mitigated by pretreatment with LIPUS. We also tested the mRNA expression levels of proinflammatory cytokines in frozen mice heart samples. AngII-induced IL-1β and IL-6 but not TNF-α expression decreased with LIPUS irradiation (Fig. 6b). However, not all of these indexes reached the level of the control group. Then, we found that administration of TLR4 inhibitor TAK-242, which can decrease the mRNA levels of proinflammatory cytokines, could totally mimic the role of LIPUS irradiation in AngII-induced cardiac fibrosis (Fig. 6c-d), suggesting that LIPUS irradiation could improve AngII-induced cardiac fibrosis by alleviating inflammation.

To confirm the relationship between inflammation and caveolin-1 in the anti-fibrotic effects of LIPUS irradiation in vitro, we next used rRtIL-1β or rRtIL-6 to increase the expression of proinflammatory cytokines. The results showed that both overexpression of IL-1β or IL-6 reversed the antifibrotic effects of LIPUS irradiation in vitro, but had insignificant effects on the expression of caveolin-1 (Fig. 6e-f). Furthermore, LIPUS-induced downregulation of the expression of proinflammatory cytokines in cardiac fibroblasts was blunted by pp2 pretreatment (Fig. 6g). Taken collectively, these data suggested that LIPUS irradiation could exert its role in improving AngII-induced cardiac fibrosis via a caveolin-1-dependent pathway in vitro.

Discussion:

In our study, we proved that LIPUS irradiation could ameliorate AngII-induced cardiac fibrosis via increased expression of the mechanotransduction protein caveolin-1. We speculate that caveolin-1 might play a possible role during the pathological process of cardiac fibrosis induced by AngII administration. To our knowledge, this study demonstrates for the first time that LIPUS irradiation can improve AngII-induced cardiac fibrosis by alleviating inflammation and oxidative stress via a caveolin-1-dependent pathway.

As a well-recognized octameric peptide hormone in the RAS, AngII has been identified to promote fibroblast differentiation in a hemodynamic-dependent or independent manner by interacting with the AT1 receptor ([40, 41]). The activated differentiation of cardiac fibroblasts to myofibroblasts is characterized as the hallmark of cardiac fibrosis and is essential in enhancing mechanical stability through increasing collagen secretion and α-SMA expression during cardiac remodeling ([38, 42]). The continuous accumulation of α-SMA-expressing myofibroblasts may result in excessive deposition and remodeling of the ECM ([43]). Additionally, injury to left ventricular structure and function and activation of fetal genes including ANP, BNP, α-MHC, and β-MHC are observed in cardiac hypertrophy and are crucial pathological changes during the progression of cardiac remodeling ([44]).

LIPUS, a novel ultrasonic therapy technique, has been shown to exert its biological effects in fracture healing and tumor treatment without tissue compression, overheating, and other side effects ([45, 46]). Recently, LIPUS irradiation has been reported to suppress myocardial fibrosis induced by acute MI in animal models ([17]). Therefore, further investigations were performed to confirm whether LIPUS irradiation could ameliorate AngII-induced cardiac hypertrophy and fibrosis.

In our study, we treated AngII-stimulated rat cardiomyocytes and cardiac fibroblasts with/without LIPUS irradiation in vitro. Under the premise that ultrasound stimulation has no effect on cell apoptosis, the obtained molecular biological and immunofluorescence results showed that LIPUS irradiation could inhibit the differentiation of cardiac fibroblasts to myofibroblasts and the activation of fetal genes associated with cardiac hypertrophy except α-MHC and β-MHC in cell culture models. LIPUS irradiation slightly inhibited AngII-induced hypertrophic growth of cardiomyocytes in our study, suggesting that LIPUS has a beneficial effect on AngII-induced cardiac fibrosis that is limited to cardiac hypertrophy in vitro. Since cardiomyocytes undergo sustained electrical and mechanical activity that is important for normal contraction-relaxation cycles ([47]), we suppose that cardiac fibroblasts may be more sensitive to mechanical stimulation derived from LIPUS than cardiomyocytes, which may account for why LIPUS irradiation could ameliorate AngII-induced cardiac fibrosis but not cardiac hypertrophy in vitro. Furthermore, we mimicked AngII-induced cardiac remodeling in a mouse model using an ALZET 2004 osmotic mini-pump filled with AngII in vivo. The model was formed after chronic AngII infusion for 4 weeks, while models that did not form successfully at the end of the 2 weeks were observed from echocardiographic data (Additional file 6: Supplemental Table 2). The treatment group received LIPUS irradiation for 20 minutes every 2 days from 1 week before surgery to 4 weeks after surgery. As expected, our echocardiographic and histopathological data and molecular biological results showed that LIPUS irradiation significantly ameliorated AngII-induced cardiac structural and hemodynamic changes associated with cardiac hypertrophy and alleviated myocardial fibrosis in vivo. Unlike newborn hearts, 60−70% of cells in adult hearts are cardiac fibroblasts that play an essential role in maintaining standard heart structure, repairing a damaged heart, and transmitting mechanical and electrical signals ([48]). Regarding the different effects of LIPUS on cardiac hypertrophy in vivo and in vitro, we suggest that the ameliorated cardiac fibrosis contributes to the improved cardiac hypertrophy in vivo.

LIPUS has been reported to exert several biological effects by mechanical stimulation related to caveolae and caveolin-1. In addition to regulating signal transduction between both caveolar and noncaveolar regions, caveolae composed of a subset of lipid (membrane) rafts have been shown to respond and adapt to environmental perturbations in various physiopathologic processes ([49, 50]). Caveolin-1, a crucial integral membrane protein within caveolar membranes, can interact with and sequester various membrane signaling molecules in tissue remodeling by binding to the caveolin-1 scaffolding domain ([51, 52]). Given that cyclic mechanical stretch can reduce myofibroblast differentiation, caveolin-1 has been studied as a novel therapeutic target of fibrosis ([24, 53]). Previous reports have shown that caveolin-1 plays the antifibrotic role in negative regulation of ECM remodeling through coordinating cytoskeletal rearrangement, cell directional migration, and apoptosis ([54−56]). Due to its role in modulating TGF-β1 signaling via downregulated expression of collagen I and other proproinflammatory cytokines, caveolin-1

has also been identified to interact and interfere with the function of the TGF-β receptor ([57]). Restoring or reintroduction of caveolin-1 expression has been shown to attenuate and prevent fibrotic diseases induced by fibrotic agents such as TGF-β1 ([58, 59]). Additionally, the caveolae-mitochondria interaction has been established to have a cardioprotective effect with the regulation of mitochondrial function ([60]). However, the possible role of caveolin-1 in the treatment of LIPUS irradiation for AngII-induced cardiac fibrosis was still unknown. In our study, we found that LIPUS irradiation did increase the expression of caveolin-1 in vivo and in vitro. Except for the fact that LIPUS itself can increase the expression of caveolin-1 by mechanical stimulation, there was no difference in caveolin-1 expression in cardiac fibroblasts between the control group and the model group. However, caveolin-1 expression in the model group was significantly higher than that in the control group in frozen heart tissues. Vascular endothelial growth factor (VEGF) is crucial in compensated angiogenesis associated with maintaining cardiac function ([61]). AngII and LIPUS irradiation have been reported to induce endothelium-derived angiogenesis by different mechanisms ([18, 62]), which was in agreement with our results that increased protein expression of VEGF was found in mice hearts after AngII and/or LIPUS treatment. Given that caveolin-1 is highly expressed in the endothelium ([63]), the above reasons may explain the increased caveolin-1 expression in heart tissues in the model group. Then, after pretreatment with the caveolin-1 inhibitor pp2, the protective effects of LIPUS towards AngII-induced cardiac fibrosis were all reversed, suggesting the role of caveolin-1 in LIPUS irradiation.

AngII-induced cardiac remodeling is characterized by a pathophysiological response to chronic inflammation with progressive fibrosis ([64, 65]). In this process, an inflammatory milieu can promote the phenotypic transformation of cardiac fibroblasts ([66]). AngII is known to have a strong proinflammatory and reported profibrotic effect on facilitating the synthesis of ECM and further contributing to myocardial fibrosis with increased expression of cytokines such as IL1β, IL6, and TNF-α ([43, 67]). Furthermore, the upregulated cytokines are the primary regulators of the immune response and cardiac function by nitric oxide (NO)-dependent or independent mechanisms ([68]).

Since LIPUS has been reported to have a protective effect against oxidative stress on endothelial-mesenchymal transition ([69]), it remained to be seen whether LIPUS irradiation could exert its effects on AngII-induced cardiac fibrosis by regulating the inflammatory response. In our study, LIPUS irradiation did reduce AngII-induced release of proinflammatory cytokines in vivo and in vitro, and overexpression of both IL1β and IL6 could reverse the antifibrotic effects of LIPUS irradiation, supporting that LIPUS attenuates cardiac fibrosis following AngII administration by alleviating inflammation in vitro. Furthermore, administration of pp2 decreased the expression of proproinflammatory cytokines, while the use of rRtIL-1β or rRtIL-6 could not affect the expression of caveolin-1, suggesting that LIPUS irradiation could improve AngII-induced cardiac fibrosis via a caveolin-1-dependent pathway.

Taken together, we have partly explained the therapeutic value of LIPUS irradiation in AngII-induced cardiac fibrosis (Fig. 6h); however, we still have some limitations that need to be considered. First, compared with its effects in vivo, the beneficial effects of LIPUS irradiation on cardiac hypertrophy were rather small in cardiomyocytes. We speculate that more irradiation sessions in vivo may enhance the

protective effects of LIPUS since the cardiomyocytes may be less sensitive to mechanical stimulation derived from LIPUS than cardiac fibroblasts. Second, we have not further examined whether the effects of LIPUS irradiation observed in our study may be blunted in caveolin-1 knock-down mice. Third, regarding the molecular mechanisms, we mainly focused on the caveolin-1-mediated inflammatory response and mitochondrial oxidative stress in the present study. As several reports have shown that MAPK and other signaling pathways are closely related to LIPUS-induced biological effects, these remain to be further studied in the antifibrotic role of LIPUS irradiation.

Conclusion:

Taken together, our current study sheds light on the protective effects of LIPUS irradiation on ameliorating AngII-induced cardiac fibrosis by alleviating inflammation and oxidative stress via a caveolin-1-dependent pathway. Therefore, LIPUS irradiation may be considered a safe and noninvasive prevention therapy for cardiac fibrosis in future clinical applications.

Abbreviations

LIPUS
Low-intensity pulsed ultrasound
AngII
Angiotension II
MI
Myocardial infarction
pp2
pyrazolopyrimidine 2
RAS
Renin-angiotensin System
ECM
Extracellular Matrix
TAC
Transverse Aortic Constriction
NOS
Nitric Oxide Synthase
PBS
Phosphate-buffered Saline
NRCMs
Neonatal Rat Cardiomyocytes
NRCFs
Neonatal Rat Cardiac Fibroblasts
LVFS

Left Ventricle Fractional Shortening

LVEF

Left Ventricle Ejection Fraction

LVIDs

Left Ventricle Internal Diameters at End Systole

LVIDd

Left Ventricle Internal Diameters at End Diastole

HW/BW

Heart Weight/Body Weight

HW/TL

Heart Weight/Tibia Length

WGA

Wheat Germ Agglutinin (HE)

HE

Hematoxylin–Eosin

ANP

Atrial Natriuretic Peptide

BNP

B-type Natriuretic Peptide

β-MHC

β-myosin Heavy Chain

α-MHC

α-myosin Heavy Chain

rRtIL-1β

reconstitute the lyophilized recombinant Rat Interleukin-1β (rRtIL-1β)

rRtIL-6

reconstitute the lyophilized recombinant Rat Interleukin-6

Declarations

Ethics approval and consent to participate

All experiments with animals were conducted strictly following the University's guidelines for the Care and Use of Laboratory Animals (publicationNo.85-23, revised1996; National Institutes of Health, Bethesda, MD, United States) and were approved by the Committee on Use and Care of Experimental Animals of Nanjing Medical University (Nanjing, China).

Consent for publication

Not applicable.

Competing interests

The authors declare that they have no competing interests.

Authors' contributions

KZ performed the experimental research; KZ, TX, and WS contributed to the study design; JM, XG, JT, DZ, and XK contributed to the design and build of LIPUS; TX, LW, and TW contributed to the establishment of animal models; KZ, JZ, and XWperformed data analysis and interpretation; KZ, JZ, and CY wrote and drafted the manuscript;BZ, WS, and XK provided technical support and revised the manuscript; All authors read and approved the final manuscript.

Availability of data and materials

The authors declare that all the data supporting the findings of this study are available within the article.

References

1. Gerdes AM, Kellerman SE, Moore JA, Muffly KE, Clark LC, Reaves PY, Malec KB, McKeown PP, Schocken DD. Structural remodeling of cardiac myocytes in patients with ischemic cardiomyopathy. Circulation. 1992;86:426–30.
2. Olivetti G, Capasso JM, Meggs LG, Sonnenblick EH, Anversa P. Cellular basis of chronic ventricular remodeling after myocardial infarction in rats. Circ Res. 1991;68:856–69.
3. Bai Y, Sun X, Chu Q, Li A, Qin Y, Li Y, Yue E, Wang H, Li G, Zahra SM, et al: **Caspase-1 regulate AngII-induced cardiomyocyte hypertrophy via upregulation of IL-1beta**. *Biosci Rep* 2018.
4. Shimizu I, Minamino T. Physiological and pathological cardiac hypertrophy. J Mol Cell Cardiol. 2016;97:245–62.
5. Shiojima I, Sato K, Izumiya Y, Schiekofer S, Ito M, Liao R, Colucci WS, Walsh K. Disruption of coordinated cardiac hypertrophy and angiogenesis contributes to the transition to heart failure. J Clin Invest. 2005;115:2108–18.
6. Lunde IG, Kvaloy H, Austbo B, Christensen G, Carlson CR. Angiotensin II and norepinephrine activate specific calcineurin-dependent NFAT transcription factor isoforms in cardiomyocytes. J Appl Physiol (1985). 2011;111:1278–89.

7. Schluter KD, Wenzel S. Angiotensin II: a hormone involved in and contributing to pro-hypertrophic cardiac networks and target of anti-hypertrophic cross-talks. Pharmacol Ther. 2008;119:311–25.

8. Fabris B, Candido R, Bortoletto M, Zentilin L, Sandri M, Fior F, Toffoli B, Stebel M, Bardelli M, Belgrado D, et al. Dose and time-dependent apoptotic effects by angiotensin II infusion on left ventricular cardiomyocytes. J Hypertens. 2007;25:1481–90.

9. Mollmann H, Schmidt-Schweda S, Nef H, Mollmann S, Burstin JV, Klose S, Elsasser A, Holubarsch CJ. Contractile effects of angiotensin and endothelin in failing and non-failing human hearts. Int J Cardiol. 2007;114:34–40.

10. Kurdi M, Randon J, Cerutti C, Bricca G. Increased expression of IL-6 and LIF in the hypertrophied left ventricle of TGR(mRen2)27 and SHR rats. Mol Cell Biochem. 2005;269:95–101.

11. Nishikimi T, Maeda N, Matsuoka H. The role of natriuretic peptides in cardioprotection. Cardiovasc Res. 2006;69:318–28.

12. Rosenkranz S. TGF-beta1 and angiotensin networking in cardiac remodeling. Cardiovasc Res. 2004;63:423–32.

13. Jia L, Wang Y, Chen J, Chen W. Efficacy of focused low-intensity pulsed ultrasound therapy for the management of knee osteoarthritis: a randomized, double blind, placebo-controlled trial. Sci Rep. 2016;6:35453.

14. Saito R, Nagase T, Tateishi T, Shimizu S, Kato T, Nakagawa T, Tsutiya M. Outcome of Low-Intensity Pulsed Ultrasound (LIPUS) for Opening Wedge High Tibial Osteotomy. J Orthop Trauma. 2017;31:3.

15. Tanaka E, Kuroda S, Horiuchi S, Tabata A, El-Bialy T. Low-intensity pulsed ultrasound in dentofacial tissue engineering. Ann Biomed Eng. 2015;43:871–86.

16. ter Haar G. Therapeutic applications of ultrasound. Prog Biophys Mol Biol. 2007;93:111–29.

17. Zheng C, Wu SM, Lian H, Lin YZ, Zhuang R, Thapa S, Chen QZ, Chen YF, Lin JF. **Low-intensity pulsed ultrasound attenuates cardiac inflammation of CVB3-induced viral myocarditis via regulation of caveolin-1 and MAPK pathways**. 2019, 23:1963–1975.

18. Shindo T, Ito K, Ogata T, Hatanaka K, Kurosawa R, Eguchi K, Kagaya Y, Hanawa K, Aizawa K, Shiroto T, et al. Low-Intensity Pulsed Ultrasound Enhances Angiogenesis and Ameliorates Left Ventricular Dysfunction in a Mouse Model of Acute Myocardial Infarction. Arterioscler Thromb Vasc Biol. 2016;36:1220–9.

19. Ogata T, Ito K, Shindo T, Hatanaka K, Eguchi K, Kurosawa R, Kagaya Y, Monma Y, Ichijo S, Taki H, et al. Low-intensity pulsed ultrasound enhances angiogenesis and ameliorates contractile dysfunction of pressure-overloaded heart in mice. PLoS One. 2017;12:e0185555.

20. da Silva Junior EM, Mesquita-Ferrari RA, Franca CM, Andreo L, Bussadori SK, Fernandes KPS. Modulating effect of low intensity pulsed ultrasound on the phenotype of inflammatory cells. Biomed Pharmacother. 2017;96:1147–53.

21. Hanawa K, Ito K, Aizawa K, Shindo T, Nishimiya K, Hasebe Y, Tuburaya R, Hasegawa H, Yasuda S, Kanai H, Shimokawa H. Low-intensity pulsed ultrasound induces angiogenesis and ameliorates left

ventricular dysfunction in a porcine model of chronic myocardial ischemia. PLoS One. 2014;9:e104863.

22. Parton RG, del Pozo MA. Caveolae as plasma membrane sensors, protectors and organizers. Nat Rev Mol Cell Biol. 2013;14:98–112.

23. Parton RG. Cell biology. Life without caveolae. Science. 2001;293:2404–5.

24. Gervasio OL, Phillips WD, Cole L, Allen DG. Caveolae respond to cell stretch and contribute to stretch-induced signaling. J Cell Sci. 2011;124:3581–90.

25. Ding L, Zeng Q, Wu J, Li D, Wang H, Lu W, Jiang Z, Xu G. Caveolin1 regulates oxidative stressinduced senescence in nucleus pulposus cells primarily via the p53/p21 signaling pathway in vitro. Mol Med Rep. 2017;16:9521–7.

26. Bartholomew JN, Volonte D, Galbiati F. Caveolin-1 regulates the antagonistic pleiotropic properties of cellular senescence through a novel Mdm2/p53-mediated pathway. Cancer Res. 2009;69:2878–86.

27. Shi XY, Xiong LX, Xiao L, Meng C, Qi GY, Li WL. Downregulation of caveolin1 upregulates the expression of growth factors and regulators in coculture of fibroblasts with cancer cells. Mol Med Rep. 2016;13:744–52.

28. Sedding DG, Hermsen J, Seay U, Eickelberg O, Kummer W, Schwencke C, Strasser RH, Tillmanns H, Braun-Dullaeus RC. Caveolin-1 facilitates mechanosensitive protein kinase B (Akt) signaling in vitro and in vivo. Circ Res. 2005;96:635–42.

29. Sonveaux P, Martinive P, DeWever J, Batova Z, Daneau G, Pelat M, Ghisdal P, Gregoire V, Dessy C, Balligand JL, Feron O. Caveolin-1 expression is critical for vascular endothelial growth factor-induced ischemic hindlimb collateralization and nitric oxide-mediated angiogenesis. Circ Res. 2004;95:154–61.

30. Jokhadar SZ, Majhenc J, Svetina S, Batista U. Positioning of integrin beta1, caveolin-1 and focal adhesion kinase on the adhered membrane of spreading cells. Cell Biol Int. 2013;37:1276–84.

31. Yeo MG, Oh HJ, Cho HS, Chun JS, Marcantonio EE, Song WK. Phosphorylation of Ser 21 in Fyn regulates its kinase activity, focal adhesion targeting, and is required for cell migration. J Cell Physiol. 2011;226:236–47.

32. Wang XM, Kim HP, Song R, Choi AM. Caveolin-1 confers antiinflammatory effects in murine macrophages via the MKK3/p38 MAPK pathway. Am J Respir Cell Mol Biol. 2006;34:434–42.

33. Wang J, Chen H, Cao P, Wu X, Zang F, Shi L, Liang L, Yuan W. Inflammatory cytokines induce caveolin-1/beta-catenin signalling in rat nucleus pulposus cell apoptosis through the p38 MAPK pathway. Cell Prolif. 2016;49:362–72.

34. Tourkina E, Richard M, Oates J, Hofbauer A, Bonner M, Gooz P, Visconti R, Zhang J, Znoyko S, Hatfield CM, et al. Caveolin-1 regulates leucocyte behaviour in fibrotic lung disease. Ann Rheum Dis. 2010;69:1220–6.

35. C PC, JA R, D P-J GSP, C RM, E B. T, S H, D K: Suppression of angiotensin II-induced pathological changes in heart and kidney by the caveolin-1 scaffolding domain peptide. PLoS one. 2018;13:e0207844.

36. AC V, MT H. K C: **Isolation and cryopreservation of neonatal rat cardiomyocytes**. *Journal of visualized experiments: JoVE* 2015.

37. Q W. Y Y, P Z, Y C, C L, J C, Y W, Y L: The crucial role of activin A/ALK4 pathway in the pathogenesis of Ang-II-induced atrial fibrosis and vulnerability to atrial fibrillation. Basic Res Cardiol. 2017;112:47.

38. Nguyen TP, Qu Z, Weiss JN. Cardiac fibrosis and arrhythmogenesis: the road to repair is paved with perils. J Mol Cell Cardiol. 2014;70:83–91.

39. Suthahar N, Meijers WC, Silljé HHW, de Boer RA. From Inflammation to Fibrosis-Molecular and Cellular Mechanisms of Myocardial Tissue Remodelling and Perspectives on Differential Treatment Opportunities. Curr Heart Fail Rep. 2017;14:235–50.

40. Jia L, Li Y, Xiao C, Du J. Angiotensin II induces inflammation leading to cardiac remodeling. Front Biosci (Landmark Ed). 2012;17:221–31.

41. Gonzalez A, Lopez B, Diez J. Fibrosis in hypertensive heart disease: role of the renin-angiotensin-aldosterone system. Med Clin North Am. 2004;88:83–97.

42. Yong KW, Li Y, Huang G, Lu TJ, Safwani WK, Pingguan-Murphy B, Xu F. Mechanoregulation of cardiac myofibroblast differentiation: implications for cardiac fibrosis and therapy. Am J Physiol Heart Circ Physiol. 2015;309:H532–42.

43. She G, Ren YJ, Wang Y, Hou MC, Wang HF, Gou W, Lai BC, Lei T, Du XJ, Deng XL. KCa3.1 Channels Promote Cardiac Fibrosis Through Mediating Inflammation and Differentiation of Monocytes Into Myofibroblasts in Angiotensin II -Treated Rats. J Am Heart Assoc. 2019;8:e010418.

44. Miteva K, Van Linthout S, Pappritz K, Muller I, Spillmann F, Haag M, Stachelscheid H, Ringe J, Sittinger M, Tschope C. Human Endomyocardial Biopsy Specimen-Derived Stromal Cells Modulate Angiotensin II-Induced Cardiac Remodeling. Stem Cells Transl Med. 2016;5:1707–18.

45. Harrison A, Lin S, Pounder N, Mikuni-Takagaki Y. Mode & mechanism of low intensity pulsed ultrasound (LIPUS) in fracture repair. Ultrasonics. 2016;70:45–52.

46. Nolte P, Anderson R, Strauss E, Wang Z, Hu LY, Xu ZK, Steen RG. Heal rate of metatarsal fractures: A propensity-matching study of patients treated with low-intensity pulsed ultrasound (LIPUS) vs. surgical and other treatments. Injury-International Journal of the Care of the Injured. 2016;47:2584–90.

47. Woodcock EA, Matkovich SJ. Cardiomyocytes structure, function and associated pathologies. Int J Biochem Cell Biol. 2005;37:1746–51.

48. Porter KE, Turner NA. Cardiac fibroblasts: At the heart of myocardial remodeling. Pharmacol Ther. 2009;123:255–78.

49. Pike LJ: **Rafts defined**: a report on the Keystone Symposium on Lipid Rafts and Cell Function. *J Lipid Res* 2006, **47**:1597–1598.

50. Head BP, Insel PA. Do caveolins regulate cells by actions outside of caveolae? Trends Cell Biol. 2007;17:51–7.

51. Boscher C, Nabi IR. Caveolin-1: role in cell signaling. Adv Exp Med Biol. 2012;729:29–50.

52. Razani B, Lisanti MP. Caveolins and caveolae: molecular and functional relationships. Exp Cell Res. 2001;271:36–44.

53. Blaauboer ME, Smit TH, Hanemaaijer R, Stoop R, Everts V. Cyclic mechanical stretch reduces myofibroblast differentiation of primary lung fibroblasts. Biochem Biophys Res Commun. 2011;404:23–7.

54. Wang XM, Zhang Y, Kim HP, Zhou Z, Feghali-Bostwick CA, Liu F, Ifedigbo E, Xu X, Oury TD, Kaminski N, Choi AM. Caveolin-1: a critical regulator of lung fibrosis in idiopathic pulmonary fibrosis. J Exp Med. 2006;203:2895–906.

55. Chung JW, Kim DH, Oh MJ, Cho YH, Kim EH, Moon GJ, Ki CS, Cha J, Kim KH, Jeon P, et al. Cav-1 (Caveolin-1) and Arterial Remodeling in Adult Moyamoya Disease. Stroke. 2018;49:2597–604.

56. Nethe M, Hordijk PL. A model for phospho-caveolin-1-driven turnover of focal adhesions. Cell Adh Migr. 2011;5:59–64.

57. Razani B, Zhang XL, Bitzer M, von Gersdorff G, Bottinger EP, Lisanti MP. Caveolin-1 regulates transforming growth factor (TGF)-beta/SMAD signaling through an interaction with the TGF-beta type I receptor. J Biol Chem. 2001;276:6727–38.

58. Gvaramia D, Blaauboer ME, Hanemaaijer R, Everts V. Role of caveolin-1 in fibrotic diseases. Matrix Biol. 2013;32:307–15.

59. Liu J, Song C, Xiao Q, Hu G, Tao L, Meng J. Fluorofenidone attenuates TGF-beta1-induced lung fibroblast activation via restoring the expression of caveolin-1. Shock. 2015;43:201–7.

60. Fridolfsson HN, Kawaraguchi Y, Ali SS, Panneerselvam M, Niesman IR, Finley JC, Kellerhals SE, Migita MY, Okada H, Moreno AL, et al. Mitochondria-localized caveolin in adaptation to cellular stress and injury. Faseb j. 2012;26:4637–49.

61. Oka T, Akazawa H, Naito AT, Komuro I. Angiogenesis and cardiac hypertrophy: maintenance of cardiac function and causative roles in heart failure. Circ Res. 2014;114:565–71.

62. Chen LY, Wang X, Qu XL, Pan LN, Wang ZY, Lu YH, Hu HY. **Activation of the STAT3/microRNA-21 pathway participates in angiotensin II-induced angiogenesis**. 2019, 234:19640–19654.

63. Ito A, Shiroto T, Godo S, Saito H, Tanaka S, Ikumi Y, Kajitani S, Satoh K, Shimokawa H. Important roles of endothelial caveolin-1 in endothelium-dependent hyperpolarization and ischemic angiogenesis in mice. Am J Physiol Heart Circ Physiol. 2019;316:H900-h910.

64. Lee SB, Kalluri R. **Mechanistic connection between inflammation and fibrosis**. *Kidney Int Suppl* 2010:S22-26.

65. Boulogne M, Sadoune M, Launay JM, Baudet M, Cohen-Solal A, Logeart D. Inflammation versus mechanical stretch biomarkers over time in acutely decompensated heart failure with reduced ejection fraction. Int J Cardiol. 2017;226:53–9.

66. Turner NA, Mughal RS, Warburton P, O'Regan DJ, Ball SG, Porter KE. Mechanism of TNFalpha-induced IL-1alpha, IL-1beta and IL-6 expression in human cardiac fibroblasts: effects of statins and thiazolidinediones. Cardiovasc Res. 2007;76:81–90.

67. Duerrschmid C, Crawford JR, Reineke E, Taffet GE, Trial J, Entman ML, Haudek SB. TNF receptor 1 signaling is critically involved in mediating angiotensin-II-induced cardiac fibrosis. J Mol Cell Cardiol. 2013;57:59–67.

68. Kleinbongard P, Heusch G, Schulz R. TNFalpha in atherosclerosis, myocardial ischemia/reperfusion and heart failure. Pharmacol Ther. 2010;127:295–314.

69. Li J, Zhang Q, Ren C, Wu X, Zhang Y, Bai X, Lin Y, Li M, Fu J, Kopylov P, et al. Low-Intensity Pulsed Ultrasound Prevents the Oxidative Stress Induced Endothelial-Mesenchymal Transition in Human Aortic Endothelial Cells. Cell Physiol Biochem. 2018;45:1350–65.

Tables

Table.1: Echocardiographic data of left ventricular function at the end of 4 weeks.

Variables	The control group (n=5)	The model group (n=10)	The LIPUS control group (n=5)	The treatment group (n=10)
LVEF(%)	67.88±1.79	45.11±2.84*	66.39±1.60	54.08±2.12#
LVFS(%)	45.68±1.82	29.51±2.85*	40.98±1.94	41.80±2.37#
LVIDd(mm)	3.43±0.16	3.90±0.08*	3.50±0.09	3.83±0.17#
LVIDs(mm)	1.92±0.13	2.44±0.17*	1.99±0.15	1.93±0.21#

The mice were randomly assigned to the control group, the model group, the LIPUS control group, and the treatment group. The mice were implanted of an ALZET 2004 osmotic mini-pump filled with either AngII (2.5 mg · kg⁻1 · d⁻¹) or PBS subcutaneously under anesthesia for 4 successive weeks. The treatment group and the LIPUS control group underwent LIPUS irradiation for 20 minutes under isoflurane anesthesia every 2 days from 1 week before surgery to 4 weeks after surgery. Transthoracic echocardiographic images of mice hearts were acquired at the end of 4 weeks after surgery using an ultrasound system. The results are expressed as the mean±SEM (LVEF: left ventricular ejection fraction; LVFS: left ventricular fractional shortening; LVIDs: LV internal diameters at end systole; LVIDd: LV internal diameters at end diastole; *P<0.05 versus the control group; #p<0.05 versus the model group).
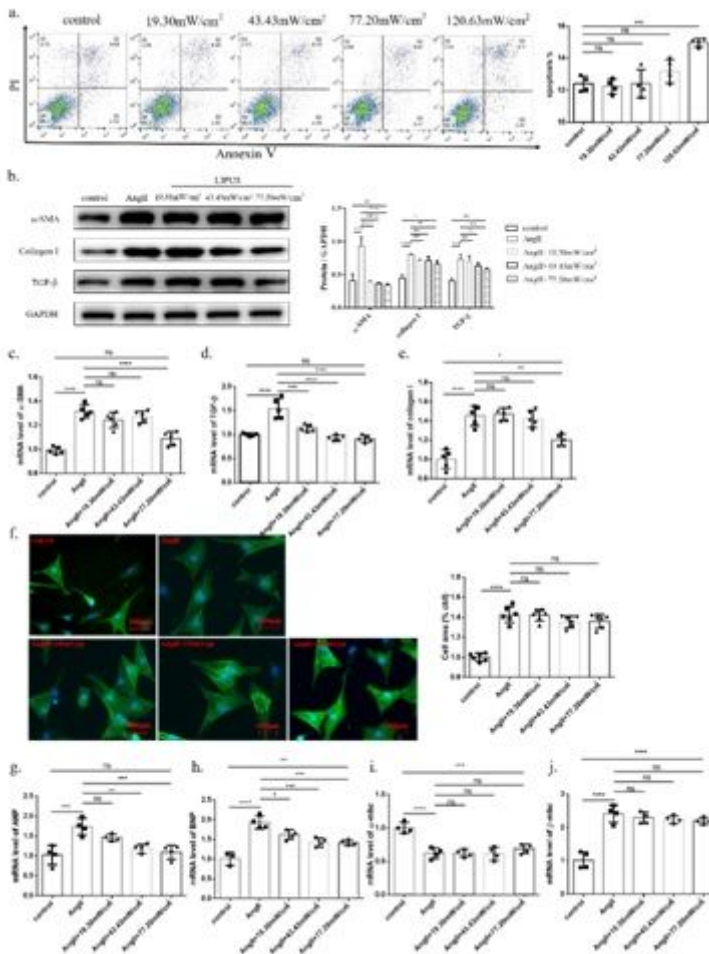
Figures

Figure 1

Effects of LIPUS irradiation on ameliorating AngII-induced cardiac fibrosis and cardiac hypertrophy in vitro. a, The results of flow cytometry on apoptosis in cardiac fibroblasts stimulated by different doses of ultrasound intensities (left) and the corresponding quantitative analysis (right). b, Protein expression levels of α-SMA, TGF-β, and collagen I as determined by western blotting (left) in cardiac fibroblasts treated with/without LIPUS irradiation and/or AngII from different groups (n>3 per group) and the corresponding densitometric analysis (right). GAPDH was detected as the loading control. c-e, mRNA expression levels of α-SMA (c), TGF-β (d), and collagen I (e) in cardiac fibroblasts from different groups determined by the qPCR method. f, Representative immunofluorescence images of cardiomyocytes labeled with α-Actinin at 400× magnification (α-Actinin, green; DAPI, blue. Scale bars, 100 μm) (left) and the corresponding quantitative analysis (right). g-j, mRNA expression levels of ANP (g), BNP (h), α-MHC (i), and β-MHC (j) in cardiomyocytes from different groups determined by the qPCR method. All mRNA expression was normalized to GAPDH, n>3. The results are expressed as the mean ± SEM (NS indicates not significant, *P<0.05, **P<0.01, ***P<0.001, compared with the control or model group).
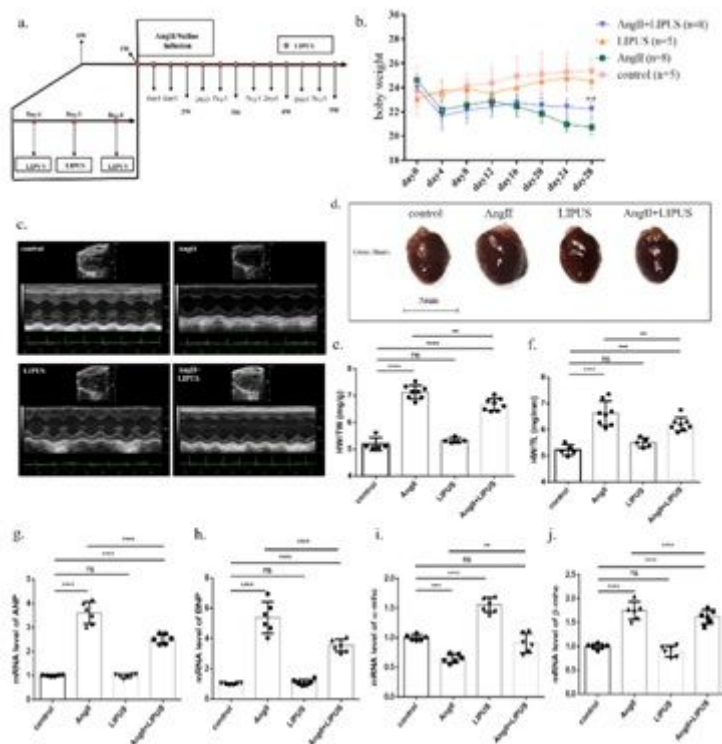
Figure 2

Effects of LIPUS irradiation on ameliorating AngII-induced cardiac hypertrophy in mice in vivo. a, Study protocol. b, Effect of LIPUS irradiation on body weight in AngII-induced mice. **P<0.01 vs AngII group. c-d, Representative M-mode echocardiography images (c) and photographs (d) of the hearts from the control group (n=5), the LIPUS control group (n=8), the model group (n=8), and the treatment group (n=5). e-f, Cardiac structure was assessed by the heart weight to total body weight (HW/TW) ratio (e) and the heart weight to tibia length (HW/TL) ratio (f) in different groups. g-j, mRNA expression levels of ANP (g), BNP (h), α-MHC (i), and β-MHC (j) in the frozen mice heart samples from indicated groups determined by the qPCR method. All mRNA expression was normalized to GAPDH, n=6. The results are expressed as the mean ± SEM (NS indicates not significant, *P<0.05, **P<0.01, ***P<0.001, ****P<0.0001, compared with the control or model group).
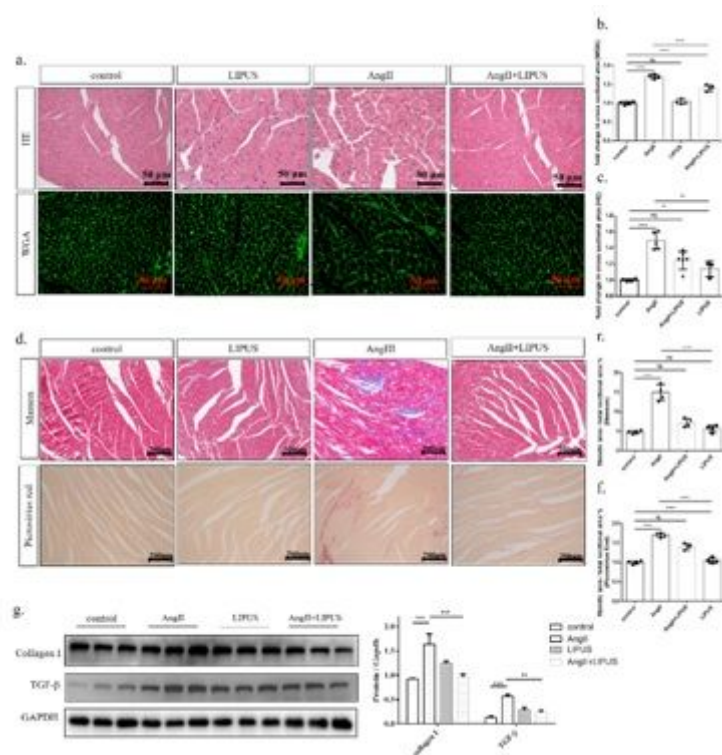
Figure 3

Effects of LIPUS irradiation on ameliorating AngII-inducedmyocardial fibrosis in mice in vivo. a, Representative images of stained longitudinal sections of LV tissue with wheat germ agglutinin (WGA, scale bar, 50 μm) (top), and hematoxylin−eosin (HE, scale bar, 50 μm) (bottom) from the different groups (n>3 per group). b-c, Quantitative analysis of the cardiomyocyte cross-sectional area stained with WGA (b) and HE (c). At least 50 cardiomyocytes per group (n>3 per group) were measured randomly using Image-Pro Plus software. d, Representative images of stained longitudinal sections of LV tissue with Masson (scale bar, 200 μm) (top) and picrosirius red (scale bar, 200 μm) (bottom) from the different groups (n>3 per group). e-f, Quantitative analysis of collagen deposition stained with Masson (e) and picrosirius red (f). g, Protein expression levels of TGF-β and collagen I in the frozen mice heart samples from different groups (n=6 per group) determined by western blotting (left) and the corresponding densitometric analysis (right). GAPDH was detected as the loading control. The results are expressed as the mean ± SEM (NS indicates not significant, *P<0.05, **P<0.01, ***P<0.001, ****P<0.0001, compared with the control or model group).
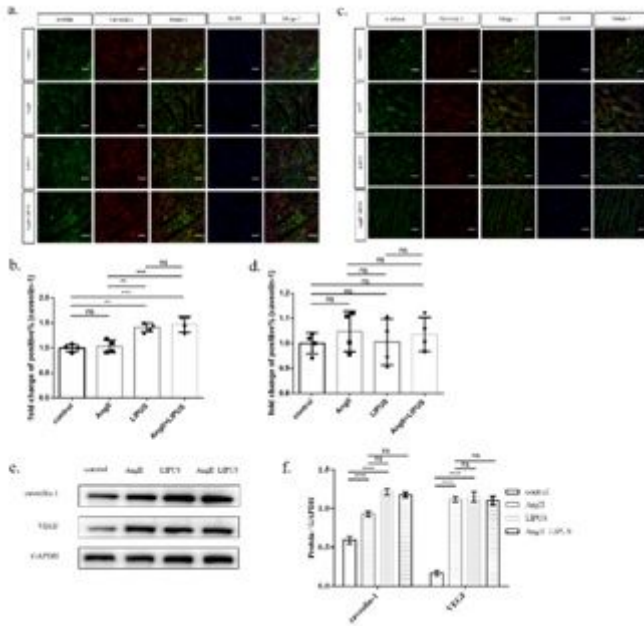
Figure 4

Role of caveolin-1 on the effects of LIPUS irradiation on ameliorating AngII-induced cardiac hypertrophyin mice in vivo. a-b, Representative immunofluorescence images of paraffin sections of LV tissue (a) labeled with caveolin-1, α-SMA, and DAPI (caveolin-1, red; α-SMA, green; DAPI, blue. Scale bars, 50 μm) and the corresponding quantitative analysis (b). c-d, Representative immunofluorescence images of paraffin sections of LV tissue (c) labeled with caveolin-1, α-Actinin, and DAPI (caveolin-1, red; α-Actinin, green; DAPI, blue. Scale bars, 50 μm) and the corresponding quantitative analysis (d). e-f, Protein expression levels of caveolin-1, and VEGF in frozen mice heart samples from the indicated groups (E) and the corresponding densitometric analysis (F); n>3 per group; GAPDH was detected as the loading control.The results are expressed as the mean ± SEM (NS indicates not significant, *P<0.05, **P<0.01, ***P<0.001, ****P<0.0001, compared with the control or model group).
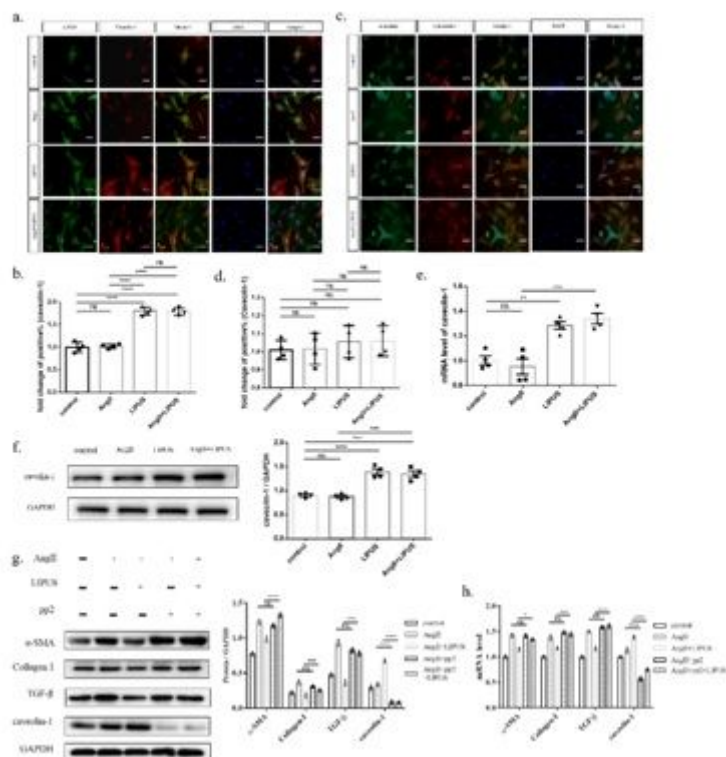
Figure 5

Role of caveolin-1 on the effects of LIPUS irradiation on ameliorating AngII-induced cardiac fibrosis in vitro. a-b, Representative immunofluorescence images of cardiac fibroblasts (a) labeled with caveolin-1, α-SMA, and DAPI (caveolin-1, red; α-SMA, green; DAPI, blue. Scale bars, 50 μm) and the corresponding quantitative analysis (b).c-d, Representative immunofluorescence images of cardiomyocytes (c) labeled with caveolin-1, α-Actinin, and DAPI (caveolin-1, red; α-Actinin, green; DAPI, blue. Scale bars, 50 μm) and the corresponding quantitative analysis (d). e-f,mRNA (e) and protein (f) expression levels of caveolin-1 in cardiac fibroblasts from different groups; n>3 per group; all mRNA and protein expressions were normalized to GAPDH. g-h, Protein (g) and mRNA (h) expression levels of caveolin-1, α-SMA, TGF-β, and Collagen I in cardiac fibroblasts from the control group, the model groups with/without pp2 pretreatment, and the LIPUS treatment groups with/without pp2 pretreatment and the corresponding densitometric analysis; n>3 per group; GAPDH was detected as the loading control.The results are expressed as the mean ± SEM (NS indicates not significant, *P<0.05, **P<0.01, ***P<0.001).
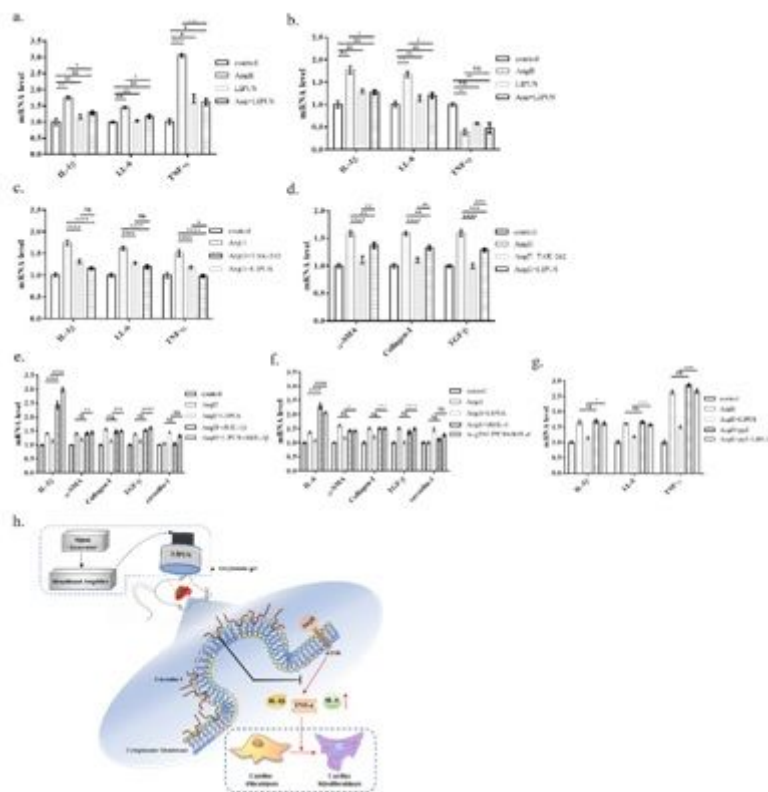
Figure 6

Relationship between inflammation and caveolin-1 in the anti-fibrotic effects of LIPUS irradiation in vitro. a-b, mRNA expression levels of IL-1β, IL-6, and TNF-α in cardiac fibroblasts (a)and frozen mice heart samples (b) from the indicated groups; n>3 per group; all mRNA expression was normalized to GAPDH. c-d, mRNA expression levels of IL-1β, IL-6, TNF-α, α-SMA, TGF-β, and Collagen I in cardiac fibroblasts from the control group, the model groups with/without TAK-242 pre-treatment, and the LIPUS treatment groups; e-f, mRNA expression levels of caveolin-1, α-SMA, TGF-β, and Collagen I in cardiac fibroblasts from the control group, the model groups with/without rRtIL-1β/ rRtIL-6 pre-treatment, and the LIPUS treatment groups with/without rRtIL-1β/ rRtIL-6 pretreatment; g, mRNA expression levels of IL-1β, IL-6, and TNF-α in cardiac fibroblasts from the control group, the model groups with/without pp2 pretreatment, and the LIPUS treatment groups with/without pp2 pretreatment. h, possible molecular mechanisms for the therapeutic effects of LIPUS are shown. n>3 per group; all mRNA expressions were normalized to GAPDH. The results are expressed as the mean ± SEM (NS indicates not significant, *P<0.05, **P<0.01, ***P<0.001).

Supplementary Files

This is a list of supplementary files associated with this preprint. Click to download.

- Additionalfile6.docx
- Supplementalmaterialslegends.docx

- Additionalfile5.docx
- Additionalfile4.docx
- Additionalfile2.docx
- Additionalfile3.docx
- Additionalfile1.docx
- personalcover.tif